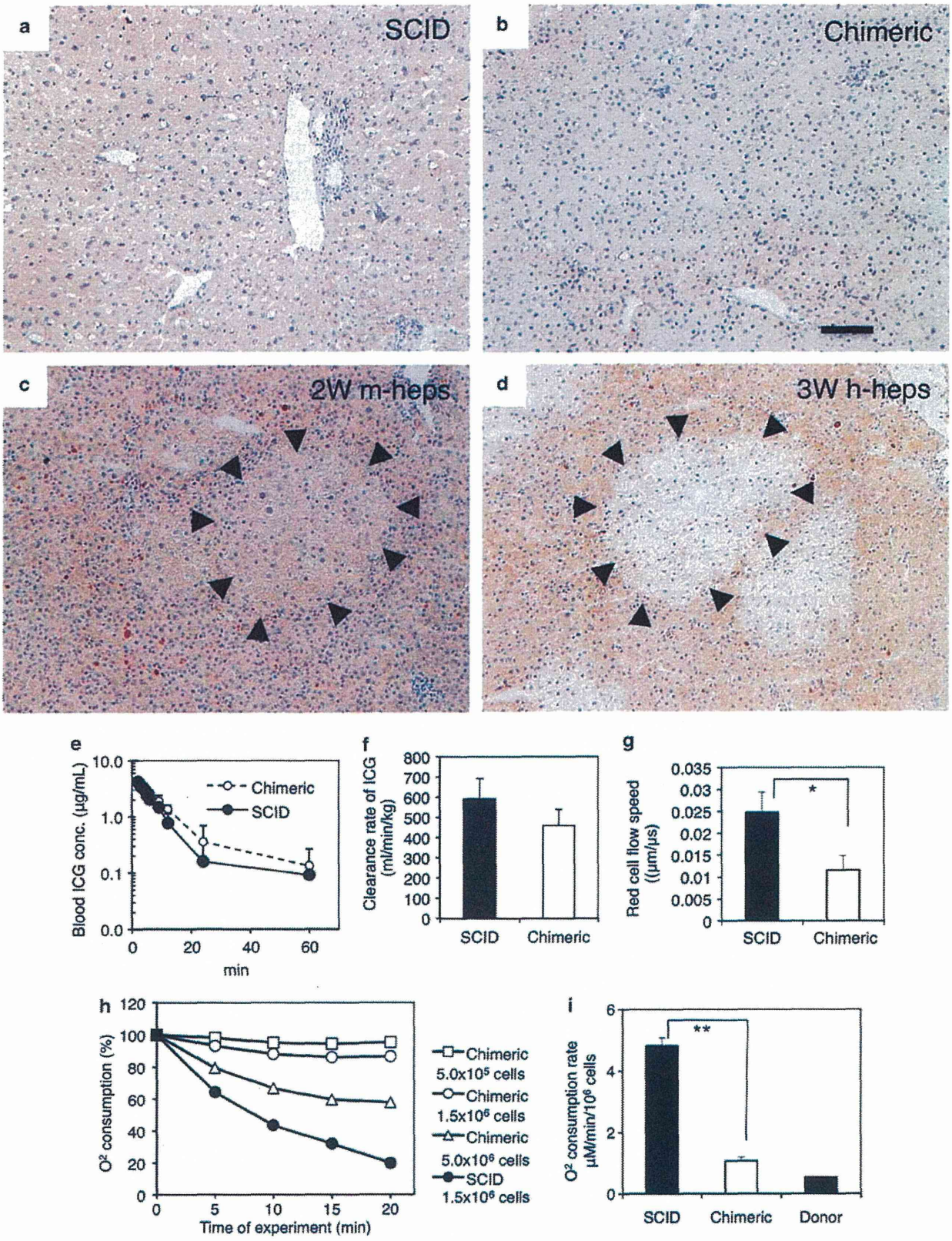
a
SCID
b
Chimeric
c
2W m-heps
d
3W h-heps
e
Blood ICG conc. (μg/mL)
10.0
1.0
0.1
0.0
Chimeric
SCID
0
20
40
60
min
f
Clearance rate of ICG (ml/min/kg)
800
700
600
500
400
300
200
100
0
SCID
Chimeric
g
Red cell flow speed ((μm/μs)
0.035
0.03
0.025
0.02
0.015
0.01
0.005
0
*
SCID
Chimeric
h
O2 consumption (%)
120
100
80
60
40
20
0
0
5
10
15
20
Time of experiment (min)
Chimeric 5.0x10^5 cells
Chimeric 1.5x10^6 cells
Chimeric 5.0x10^6 cells
SCID 1.5x10^6 cells
i
O2 consumption rate μM/min/10^6 cells
6
4
2
0
**
SCID
Chimeric
Donor

junctions, and desmosomes, directly adjoined bile canaliculi between h-heps (Figure 7a). In rare cases, bile canaliculi were also formed between h-heps and m-heps (Figure 7b). In the peripheral areas of the cytoplasm in groupings of two h-heps and one m-hep, many microvilli projected into the intercellular clefts on the lateral aspects of the hepatocytes (Figure 7c). A small number of cone-like cytoplasmic processes formed contacts with neighboring cells, not only between h-heps (Figure 7c) but also between m-heps and h-heps (Figure 7d). Electron microscopic observation showed gap junctions between h-heps (Figure 7e) and between m-heps (data not shown).

Changes in Blood Biochemistry by Repopulation of Mouse Liver with H-Heps

Sera of the chimeric (Table 1a), uPA/SCID, and SCID mice were biochemically tested (Table 3). The data for the normal range in humans[21,22] are also shown in Table 3. GOT and GPT were higher in the chimeric and uPA/SCID mice than in the normal mice because of the liver damage by uPA expression in the m-heps.[2] GGT was significantly higher in the chimeric mice than in the SCID mice and the normal human samples.[21] CHE activity differed between humans and male SCID mice (660–1620 IU/l[22] and 18 IU/l, respectively). CHE activity in the male chimeric mice was ~400 IU/l. These data indicate that the c-heps synthesized and secreted GGT and CHE in the same manner as human hepatocytes. HDL-c and low-density lipoprotein cholesterol (LDL-c) ratios also differed between humans and mice. HDL-c was higher than LDL-c in the SCID mice, whereas LDL-c was higher than HDL-c in humans.[22] LDL-c was higher than HDL-c in the chimeric mice (data not shown), but the HDL-c value was lower than that of normal humans (Table 3). ALB was higher in humans than in mice. Similarly, ALB was higher in the chimeric mice than in the SCID mice, indicating that the sera in the chimeric mice may have been acquiring human characteristics. The biomarkers BUN, TCHO, TG, TBIL, GLU, and TP did not significantly differ between male chimeric and male SCID mice.

Comparison of Gene Expression Profiles in Hepatocytes Isolated from Chimeric Mouse and Human Livers

The mRNA expression profiles of c-heps and h-heps were compared. The c-heps were isolated from three 9MM- and 6YF-chimeric mice (Table 1a), whereas h-heps were isolated from four human liver tissues (Table 1b). The gene profiles were determined for the two types of hepatocytes using microarrays representing 54 675 human transcripts. Among these, 16 605 transcripts (30% of total probes) were assigned as present (P flag) for either all of the c-heps or all of h-heps, and 81.9% were expressed at similar levels (<2-fold difference) in the two types of hepatocytes.

The data for c-heps and h-heps (25YF, 28YM, 57YM, and 61YF) and the 22 h-tissues were clustered for 46 336 probes. The cluster analysis showed that 6 c-heps formed a cluster, and the 4 h-heps and h-liver formed another cluster, with these two clusters closest among the h-tissues (Supplementary Figure 1). PCA was performed for 46 336 probes. PCA showed that the 6 c-heps and 4 h-heps were extremely close to each other, and that the h-liver was the closest to the cluster of the 6 c-heps and 4 h-heps among h-tissues (Figure 8a). We also performed cluster analysis using the 685 liver high signature probes and the 805 liver low signature probes for c-heps, h-heps, and the 22 h-tissues. The cluster analysis demonstrated a close association among c-heps, h-heps, and h-liver (Figure 8b). Pearson's correlation coefficient was calculated for the expression levels of the liver-specific genes (685 probes), resulting in 0.812–0.909 for h-heps *vs* c-heps, 0.881–0.959 for h-heps *vs* h-heps, and 0.903–0.970 for c-heps *vs* c-heps.

The ratios of gene expression levels in the c-heps to those in the h-heps were compared using the data from the microarray and real-time qRT-PCR analyses. The expression levels of 17 genes were divided according to those of h-*GAPDH*. The microarray and real-time qRT-PCR data were well correlated (Spearman's correlation coefficient by rank test = 0.975; Figure 8c).

Moreover, of the 16 605 transcripts, 436 transcripts (2.6%) were twofold lower in expression in the c-heps than in the h-heps ($P<0.05$, two-sided Welch's *t*-test). Of the same total, 197 transcripts (1.2%) showed twofold greater expression in the c-heps than in the h-heps ($P<0.05$; Supplementary Table 3).

DISCUSSION

We morphometrically determined the structure of chimeric mouse livers, clarified the ratios of their component cells (heps, Kupffer cells, SECs, and stellate cells), and determined their morphological relationships through immunohistochemistry and electron microscopy. We recently reported that BrdU incorporation into h-heps was ~6% at 2 or 3 weeks after transplantation, had decreased thereafter, and had dropped to ~2% at 7 and 9 weeks after transplantation. At 11 weeks after transplantation, BrdU

Figure 5 Ultrastructure of the chimeric mouse livers as revealed by TEM (**a–e**) and SEM (**f**). The h-heps contained abundant glycogen and the presence of lipid droplets (**a, d**), whereas the mouse hepatocytes damaged by uPA expression showed an abundance of small granules (indicated by the arrow in the inset; **b**). The mouse hepatocytes normalized by deletion of the uPA gene showed a normal structure (**c**). Bile canaliculi formed on the apical membranes of adjacent human hepatocytes, (**d**) and sinusoidal structures were observed on the basal cell membranes (**a, d**). A hepatic stellate cell containing lipid droplets was observed in the space of Disse (**e**). Fenestration was normally seen on SECs (**f**). Bar indicates 1 μm in (**a–c, e, f**); 0.5 μm in the squares of (**b**); and 5 μm in (**d**). BC, bile canaliculi; BL, blood cell; HSC, hepatic stellate cell; L, lipid droplets; M, mitochondria; SD, sinusoid; SEC, sinusoidal endothelial cell.

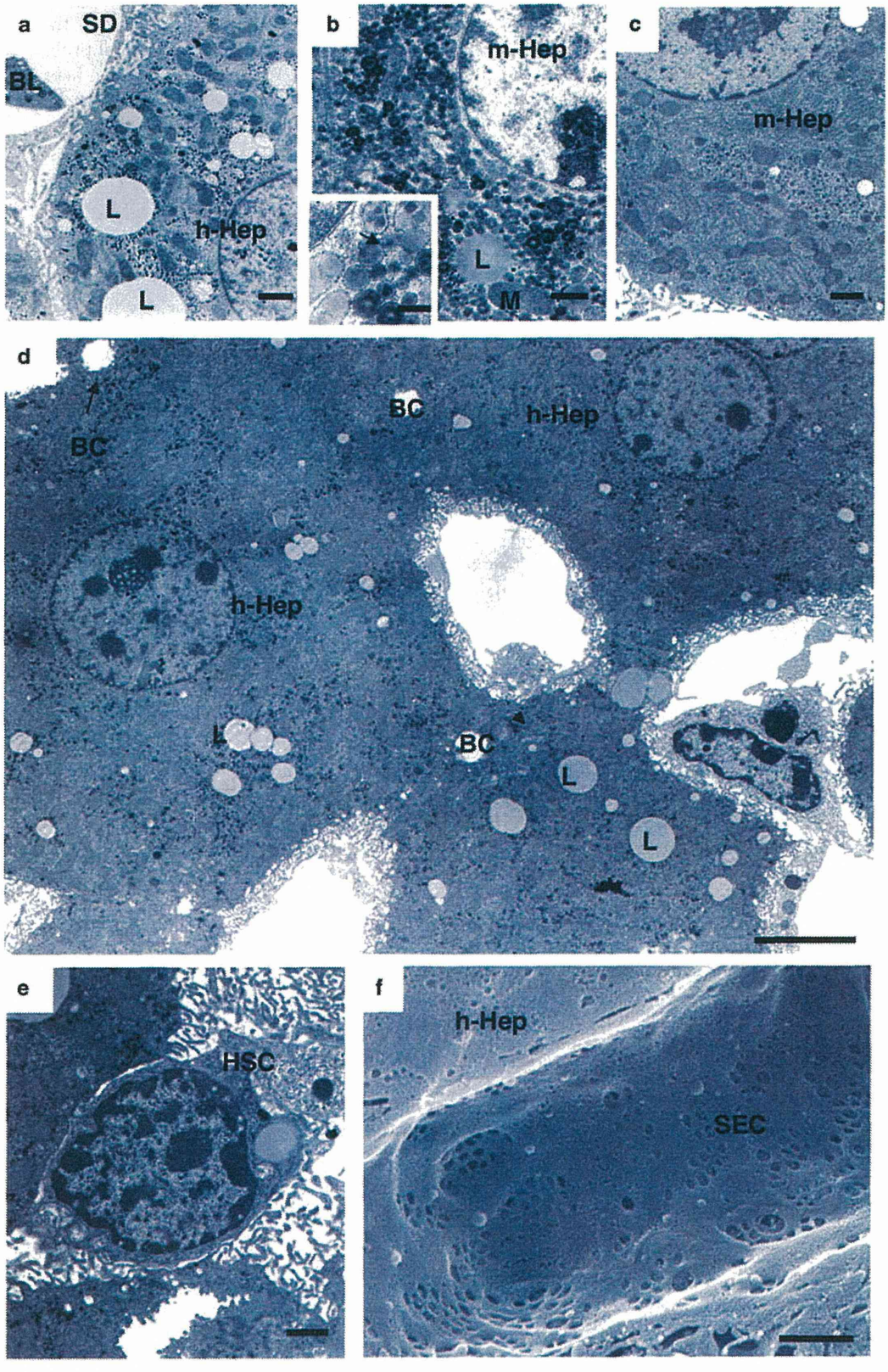
a
SD
BL
L
h-Hep
L
b
m-Hep
L
M
c
m-Hep
d
BC
BC
h-Hep
h-Hep
L
BC
L
L
e
HSC
f
h-Hep
SEC

incorporation was ~1%, which was the same as the control level in adult SCID mouse livers.[20] We also demonstrated that the liver weight to body weight ratios of chimeric mouse livers were ~2 times greater than those of normal mice when the transplants terminated proliferation.[20] These results were considered to indicate hyperplasia of the h-heps, as no significant differences in cell size were observed.[20] The mRNAs of proliferating h-heps contained lower levels of TGF-β type I receptors (TGFBR1), TGFBR2, and activin A type IIA receptors (ACVR2A) than that of resting h-heps from human livers (normal levels), and these levels remained low when the transplants terminated proliferation.[20] Therefore, we suggested that the chimeric mouse livers terminated their growth because of contact inhibition of h-heps or other mechanisms without the TGF-β signaling pathway. From these data, we determined that the h-heps in the chimeric mouse livers were not completely in the G0 stage. The h-heps in the chimeric mouse livers showed twin-cell plates, indicating that some of the proliferating features continued as in regenerating or neonatal livers.[20] In the present study, the morphometric analysis revealed similar HSC ratios in chimeric and SCID mice but an h-hep ratio in the chimeric mouse livers that was twofold higher than that in the SCID mouse liver, corresponding to the twin-cell plates in the chimeric mouse liver. The liver blood flow rate was similar between the SCID and chimeric mice. On the other hand, sinusoidal blood flow in the chimeric mouse was approximately one-half of that in the SCID mouse, probably because of the enlargement of the chimeric mouse liver. However, no disorders in the microcirculation of the chimeric mouse liver were observed. The oxygen consumption rate of hepatocytes is known to be negatively correlated with the average body weights of different species.[23] Using a formula showing the relationship between resting hepatocyte oxygen consumption (y) and body weight (x) ($y = 7.09x$),[23] the ratio of the hepatocyte oxygen consumption of mouse (body weight: 0.02 kg) to that of human (body weight: 60 kg) is ~5. In the present study, the oxygen consumption of h-heps was 1/4.5 of m-heps, which was very close to the above calculated rate.

After partial hepatectomy, the division of heps resulted in twin-cell plates, and the heps subsequently showed hypoxia.[24] HIF-1 induction induced expression of downstream genes, such as VEGF and TGF-β3.[24] The author suggested that hypoxia of the heps induced reconstruction from twin-cell plates into single-cell plates by growth of the SECs.[24] hHIF-1α, hVEGF, and hTGF-β3 mRNA expression levels in the chimeric mouse livers were lower than those in human livers by real-time qRT-PCR (data not shown). In the present study, no evidence was found that the h-heps showed hypoxia in the chimeric mouse liver. This finding suggests that the h-heps in the chimeric mice may not be hypoxic, even in the twin-cell plates, because of low oxygen consumption in these cells.

With electron microscopic observation, we were able to easily distinguish h-heps from m-heps in the white areas because of the highly expressed uPA gene. The h-heps showed abundant glycogen and large lipid droplets, whereas m-heps in the white areas had abundant small vesicles in the cytoplasm. Distinguishing h-heps from m-heps in the red areas was difficult because of the deletion of the uPA gene. M-heps retained quantities of glycogen particles, and careful observation of m-heps in the red areas revealed prominent peroxisomes and fewer lipid droplets in the uPA-gene-deleted m-heps than in the h-heps. On the other hand, very few peroxisomes were present in the h-heps. Junctional complexes and bile canaliculi were frequently observed between h-heps in the chimeric mouse livers. In rare cases, bile canaliculi were formed between h-heps and m-heps. In the peripheral cytoplasmic areas of two adjacent h-heps or a h-hep and a m-hep, abundant microvilli projected into the intercellular clefts on the lateral aspects of the hepatocytes. These characteristic morphological features have been frequently observed in regenerating livers.[25] The formation of junctional complexes and bile canaliculi between m-heps and h-heps is an important finding that demonstrates the ability of the mouse bile duct system to extract bile produced by the h-heps. Electron microscopic examination further revealed that SECs and stellate cells existed normally along hepatic cell plates. Fenestration was observed on the SECs in the chimeric mouse livers. These results indicate that chimeric mouse livers showed twin-cell plates like those often seen in regenerating and neonatal livers, whereas h-heps and m-HSCs were normally reconstructed in the chimeric mouse livers.

The present study is the first to compare the gene expression patterns of c-heps and h-heps using microarray analysis. Approximately 82% were expressed at similar levels (<2-fold difference) in the two types of hepatocytes. There was the possibility that mouse transcripts were also included as cDNAs hybridized in the currently adopted microarray assay. Our previous study indicated that the RI represented a lower estimation of the real h-hepatocyte purity in hepatocyte preparations because m-heps were often lost during collagenase digestion because of fragility against the enzyme. The correct h-hepatocyte purity in the c-heps was $90.8 \pm 6.4\%$ ($n = 10$).[17] We further checked the cross-hybridization of the cDNAs of the mouse livers and found that 5643 of 54 675 (10.3%) transcripts were positive. As a whole, the presence of m-heps in the c-heps at <10% did not affect the microarray assays in the present study.[17] PCA and cluster analyses showed that the gene expression patterns of the c-heps were extremely similar to those of the h-heps. These data support our previous finding that c-heps retain phenotypes similar to those of h-heps, including *P*450 (CYP), phase II enzymes, and transporters.[2–4] The c-hep samples and h-hep samples are clearly distinct with the 'normal' liver. One possible explanation is that the normal liver tissue contains both h-heps and h-HSCs. Using Fisher's test, we also analyzed 46 336 probes that were assigned as

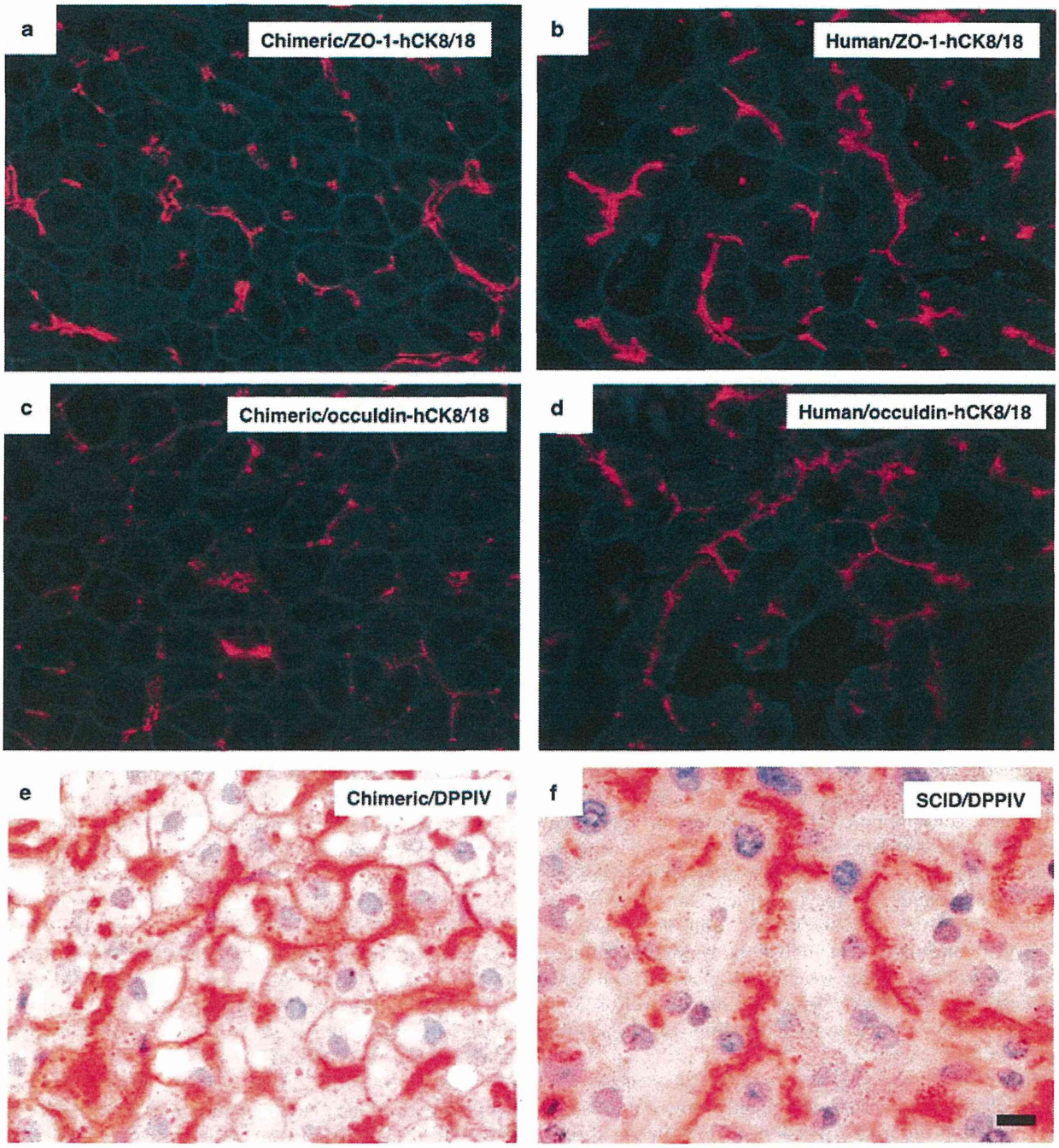

Figure 6 Immunohistochemistry of proteins related to cell adherence in human and chimeric mouse livers, and enzyme histochemistry of DPPIV in SCID and chimeric mouse livers. 9MM-chimeric mouse and human liver sections were stained with ZO-1 (**a**, **b**) and occludin (**c**, **d**) antibodies and stained for DPPIV (**e**, **f**). These proteins were located between hepatocytes in the chimeric mouse livers (**a**, **c**) and the human livers (**b**, **d**). Fewer occludin deposits were observed in the chimeric mouse livers (**c**) than in the human livers (**d**). DPPIV-positive signals were located on the basal membranes in the SCID mice (**f**), but were also observed at the peripheries of human hepatocytes in chimeric mice (**e**). Bar = 10 μm. Magnification is the same in all panels.

positive (P flag) for at least one of the flags in any of the c-heps, h-heps, or 22 h-tissues (Supplementary Table 4). The overlap *P*-values and odds ratio were determined between the liver signature probes and the probes of the h-heps with signals more than 2 times higher or lower compared with the average signals of all the tissues. The number of overlap probes were found to be 539–642 among 685 probes in the liver high expression signature, and the overlap *P*-values in the liver high

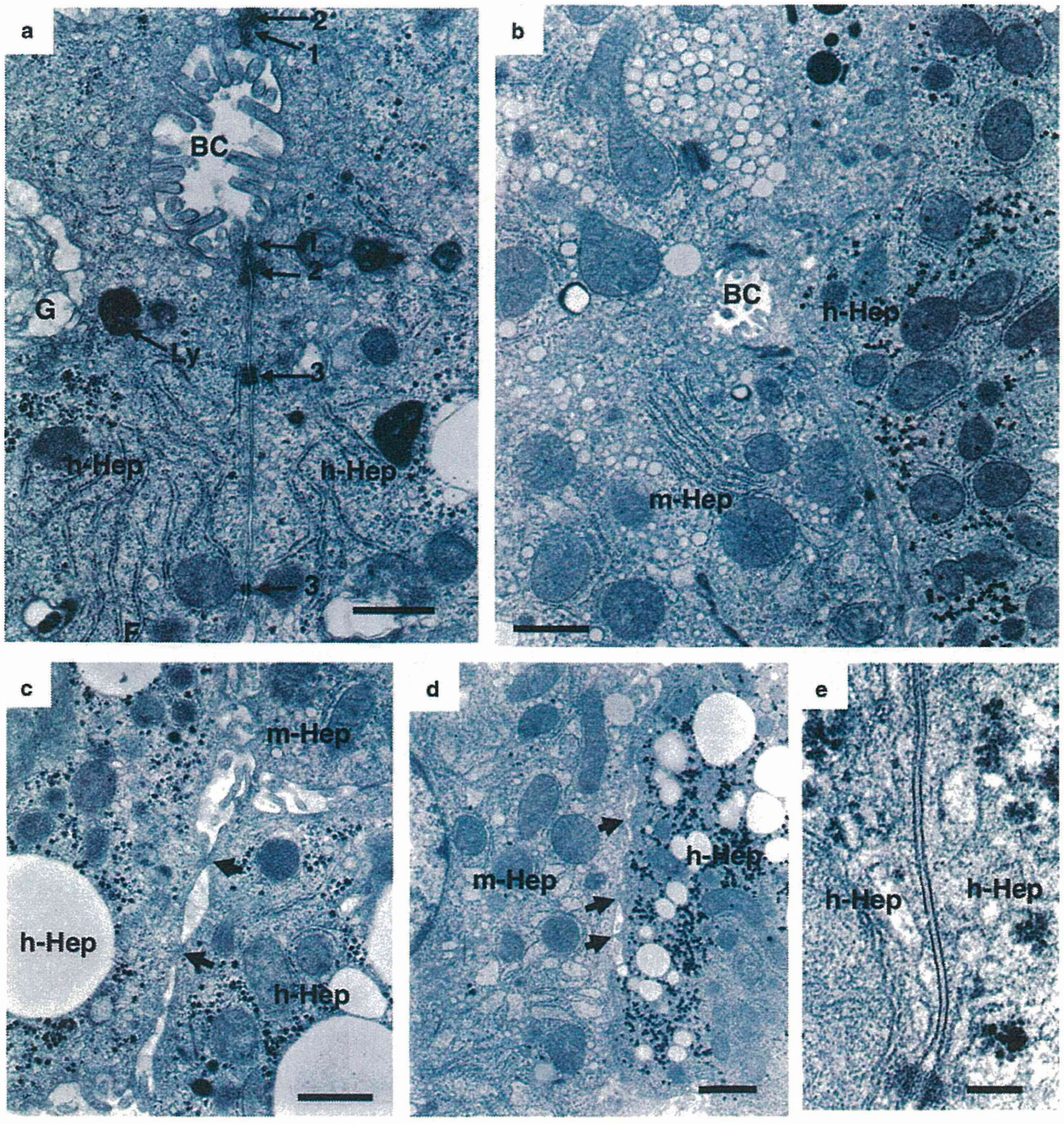

Figure 7 Ultrastructure of cell–cell contact in the chimeric mouse livers. Bile canaliculi were observed between adjacent h-heps (**a**) and between h- and m-heps (**b**) in the 4YF-chimeric mouse liver, as well as junctional complexes (tight junction, 1; adherence junction, 2; desmosome, 3). In the peripheral cytoplasmic areas of groups formed by two adjacent human hepatocytes and one m-hep, many microvilli projected into the intercellular clefts on the lateral aspects of the hepatocytes (**c**). We judged that the left and right cells in (**b**) are m-hep damaged by uPA expression and h-hep, respectively, because many membrane-limited granules are scattered throughout the cytoplasm in the left cell and the presence of abundant glycogen particles is observed in the cytoplasm in the right cell. A small number of cone-like cytoplasmic processes made contact with neighboring cells (**c, d**). Gap junctions were frequently observed between human hepatocytes (**e**). Bar = 0.5 μm in (**a**); 1 μm in (**b, c, d**); and 0.1 μm in (**e**). BC, bile canaliculi; G, Golgi complex; Ly, lysosome.

expression signature were $<2.2 \times 10^{-16}$. The number of overlap probes were 153–485 among 805 probes in the liver low expression signature and were fewer than in the liver high expression signature; however, the overlap *P*-values in the liver low expression signature were also $<2.2 \times 10^{-16}$. From these data, we observe that the c-hep samples, h-hep samples,

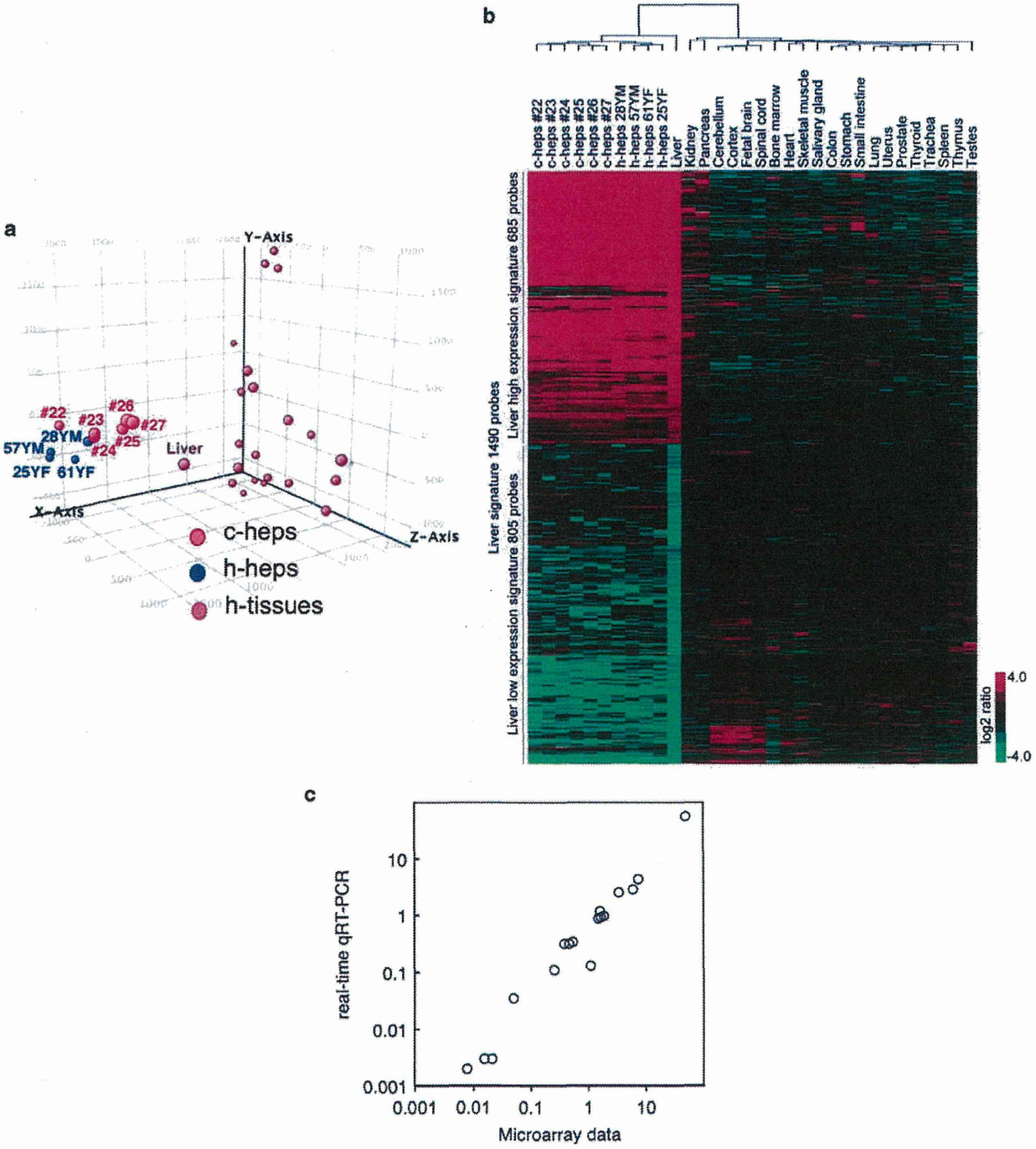

Figure 8 Similarity of gene expression between c-heps and h-heps. (**a**) PCA of c-heps, h-heps, and 22 h-organs or tissues. (**b**) Cluster analysis using the 685 liver high signature probes and the 805 liver low signature probes for c-heps, h-heps, and 22 h-tissues. (**c**) Comparison of the gene expression profiles of chimeric and human hepatocytes using microarray and real-time qRT-PCR analyses. The ratios of gene expression in c- and h-heps, as obtained from the microarray analysis and real-time qRT-PCR, were compared for 17 genes. These data were well correlated.

and liver are highly similar, particularly in the liver high signature probes, but the differences in the expression levels of the liver low signature probes resulted in the clear distinction of the c-hep samples and h-hep samples with the 'normal' liver.

Microarray analysis showed that 191 (170 genes) and 436 (320 genes) probes were significantly (>2 times) higher and lower, respectively, in c-heps than in h-heps. These genes may be up- and down-regulated in the chimeric mouse livers, probably by mismatched receptor–ligand combinations

Table 3 Blood chemistry of chimeric, uPA/SCID, and uPA (wt/wt)/SCID mice

Sex		Chimeric		uPA/SCID	SCID	Human (reference value,
		Male	Female	Male	Male	Male and female)
Age (w)		13.4 ± 0.9	12.0 ± 1.9	12.0 ± 0.0	11.0 ± 0.0	—
Body weight		17.3 ± 2.3	17.6 ± 1.7	17.4 ± 0.3	27.3 ± 0.9	—
n		*5*	*5*	*5*	*3*	—
GOT	U/l	214.6 ± 75.1**[a]	126.8 ± 72.5	367.6 ± 107.7**[b]	44.0 ± 23.3	20–48[c]
GPT	U/l	98.6 ± 16.8*[a]	58.6 ± 18.0	176.4 ± 28.9**[b]	44.3 ± 37.7	10–40[c]
GGT	U/l	23.0 ± 4.6**[a]	15.0 ± 3.9	1.2 ± 0.4	3.7 ± 4.6	0–30[c]
CHE	U/l	396.8 ± 80.2**[a]	282.2 ± 34.1	42.6 ± 8.0**[b]	18.0 ± 5.2	660–1620[d]
BUN	mg/dl	27.3 + 4.0	23.2 ± 4.6	24.6 ± 9.1	25.3 ± 3.9	8–23[c]
TCHO	mg/dl	88.0 ± 25.8	69.6 ± 18.7	56.8 ± 6.8**[b]	83.3 ± 2.5	<200[c]
HDL-c	mg/dl	20.2 ± 3.4**[a]	18.8 ± 3.7	52.4 ± 7.0**[b]	72.7 ± 6.8	35–80[c]
TG	mg/dl	129.2 ± 24.6	133.2 ± 13.8	82.2 ± 11.0	99.3 ± 10.2	10–190[c]
TBIL	mg/dl	0.4 ± 0.1	0.4 ± 0.0	0.5 ± 0.2	0.6 ± 0.5	0.3–1.2[c]
GLU	mg/dl	154.6 ± 21.6	148.8 ± 31.9	116.4 ± 30.5	154.7 ± 14.2	70–110[c]
ALB	g/dl	3.0 ± 0.4*[a]	2.4 ± 0.1	1.7 ± 0.3	2.2 ± 0.3	3.5–5.0[c]
TP	g/dl	5.0 ± 0.7	4.2 ± 0.3	3.5 ± 0.7*[c]	5.3 ± 0.6	6.0–8.0[c]

[a]Chimeric mouse (male) *vs* SCID mouse (male).
[b]uPA/SCID mouse (male) *vs* SCID mouse (male).
[c]Reference number.[21]
[d]Reference number.[22]
*$P<0.05$, **$P<0.01$.

because of species differences. For example, h-heps were considered to be deficient in growth hormone (GH) because the hGH receptor (hGHR) was unresponsive to mouse GH.[26] Human insulin-like growth factor 1 (IGF-1) was undetectable in chimeric mouse sera.[17,27] We recently identified 4 downregulated and 14 upregulated genes in the chimeric mouse livers when they were treated with hGH.[17] In this microarray analysis, the expression level of fatty acid desaturase 1 (FADS1, c-heps/h-heps ratio: 20.225) was significantly higher in c-hep than in h-heps (Supplementary Table 3). Meanwhile, the expression levels of IGF-1 (c-heps/h-heps ratio: 0.002), suppressors of cytokine signaling 2 (SOCS2; 0.012 and 0.030), nicotinamide *N*-methyltransferase (NNMT; 0.025 and 0.019) chromosome 5 open reading frame 13 (C5orF13; 0.345), solute carrier family 16, member 1(SLC16A1; 0.485 and 0.432), steroid-5-α-reductase, and α-polypeptide 1 (SRD5A1; 0.486 and 0.461) were significantly lower in c-heps (Supplementary Table 3). Consequently, 1 of 170 genes and 6 of 320 genes were up- and down-regulated in c-heps, respectively, because of the lack of hGH in the sera.

Biochemical testing of the chimeric mouse sera revealed high GOT and GPT levels in chimeric and uPA/SCID mice, probably because of m-hep damage caused by uPA expression.[2,28] CHE was higher in chimeric mice than in uPA/SCID and SCID mice, which may be a result of the influence of typically higher h-hep CHE levels. Serum HDL-c levels are higher in mice than in humans, because mice lack cholesterol ester transport proteins that convert HDL-c to LDL-c.[29] HDL-c was lower in the chimeric mice than in the uPA/SCID mice, SCID mice, and humans. At present, the reason for the low HDL-c levels in the chimeric mice is not clear. Further investigations are needed to resolve this question.

We conclude that the chimeric mouse livers showed nearly normal morphology and expressed most genes at similar levels as normal human livers.

Supplementary Information accompanies the paper on the Laboratory Investigation website (http://www.laboratoryinvestigation.org)

ACKNOWLEDGEMENTS
A part of this research was supported by the Yoshizato Project of the Cooperative Link of Unique Science and Technology for Economic Revitalization (CLUSTER), Japan. We thank Y Yoshizane and R Inoue from PhoenixBio, and H Kohno, Y Matsumoto, and S Nagai from CLUSTER for their technical assistance. We also thank H Duimel, University Maastricht, for preparation of the SEM specimen.

DISCLOSURE/CONFLICT OF INTEREST
The authors declare no conflict of interest.

1. Dalvie D, Obach RS, Kang P, *et al.* Assessment of three human in vitro systems in the generation of major human excretory and circulating metabolites. Chem Res Toxicol 2009;22:357–368.

2. Tateno C, Yoshizane Y, Saitou N, *et al.* Near completely humanized liver in mice shows human-type metabolic responses to drugs. Am J Pathol 2004;165:901–912.
3. Katoh M, Matsui T, Okamura H, *et al.* Expression of human phase II enzymes in chimeric mice with humanized liver. Drug Metab Dispos 2005;33:1333–1340.
4. Nishimura M, Yoshitsugu H, Yokoi T, *et al.* Evaluation of mRNA expression of human drug-metabolising enzymes and transporters in chimeric mouse with humanized liver. Xenobiotica 2005;35: 877–890.
5. Shi J, Fujieda H, Kokubo Y, *et al.* Apoptosis of neutrophils and their elimination by Kupffer cells in rat liver. Hepatology 1996;24: 1256–1263.
6. Warren A, Le Couteur DG, Fraser R, *et al.* T lymphocytes interact with hepatocytes through fenestrations in murine liver sinusoidal endothelial cells. Hepatology 2006;44:1182–1190.
7. Sato Y, Yamada H, Iwasaki K, *et al.* Human hepatocytes can repopulate mouse liver: histopathology of the liver in human hepatocyte-transplanted chimeric mice and toxicologic responses to acetaminophen. Toxicol Pathol 2008;36:581–591.
8. Meuleman P, Libbrecht L, De Vos R, *et al.* Morphological and biochemical characterization of a human liver in a uPA-SCID mouse chimera. Hepatology 2005;41:847–856.
9. Nonaka H, Tanaka M, Suzuki K, *et al.* Development of murine hepatic sinusoidal endothelial cells characterized by the expression of hyaluronan receptors. Dev Dyn 2007;236:2258–2267.
10. Katayama S, Tateno C, Asahara T, *et al.* Size-dependent in vivo growth potential of adult rat hepatocytes. Am J Pathol 2001;158: 97–105.
11. Ban D, Kudo A, Sui S, *et al.* Decreased Mrp2-dependent bile flow in the after-warm ischemic rat liver. J Surg Res 2009;153:310–316.
12. Mabuchi A, Wake K, Marlini M, *et al.* Protection by glycyrrhizin against warm ischemia-reperfusion-induced cellular injury and derangement of the microcirculatory blood flow in the rat liver. Microcirculation 2009;16:364–376.
13. Wisse E, Braet F, Duimel H, *et al.* Fixation methods for electron microscopy of human and other liver. World J Gastroenterol 2010;16:2851–2866.
14. Seglen PO. Preparation of isolated rat liver cells. Methods Cell Biol 1976;13:29–83.
15. Bolstad BM, Irizarry RA, Astrand M, *et al.* A comparison of normalization methods for high density oligonucleotide array data based on variance and bias. Bioinformatics 2003;19:185–193.
16. Eisen MB, Spellman PT, Brown PO, *et al.* Cluster analysis and display of genome-wide expression patterns. Proc Natl Acad Sci USA 1988;95:14863–14868.
17. Tateno C, Kataoka M, Utoh R, *et al.* Growth hormone-dependent pathogenesis of human hepatic steatosis in a novel mouse model bearing a human hepatocyte-repopulated liver. Endocrinology 2011;152:1479–1491.
18. Asahina K, Sato H, Yamasaki C, *et al.* Pleiotrophin/HB-GAM as a mitogen of rat hepatocytes and its role in regeneration and development of liver. Am J Pathol 2002;160:2191–2205.
19. Benjamini Y, Hochberg Y. Controlling the false discovery rate: a practical and powerful approach to multiple testing. J Roy Statist Soc Ser B 1995;57:289–300.
20. Utoh R, Tateno C, Kataoka M, *et al.* Hepatic hyperplasia associated with discordant xenogeneic parenchymal-nonparenchymal interactions in human hepatocyte-repopulated mice. Am J Pathol 2010;177:654–665.
21. Michael L. Laboratory Medicine: The Diagnosis in the Clinical Laboratory, New York, 2010.
22. Jensen FS, Skovgaard LT, Viby-Mogensen J. Identification of human plasma cholinesterase variants in 6,688 individuals using biochemical analysis. Acta Anaesthesiol Scand 1995;39:157–162.
23. Porter RK, Brand MD. Causes of differences in respiration rate of hepatocytes from mammals of different body mass. Am J Physiol 1995;269:R1213–R1224.
24. Maeno H, Ono T, Dhar DK, *et al.* Expression of hypoxia inducible factor-1alpha during liver regeneration induced by partial hepatectomy in rats. Liver Int 2005;25:1002–1009.
25. Tomoyori T, Ogawa K, Mori M, *et al.* Ultrastructural changes in the bile canaliculi and the lateral surfaces of rat hepatocytes during restorative proliferation. Virchows Arch B Cell Pathol Incl Mol Pathol 1983;42: 201–211.
26. Souza SC, Frick GP, Wang X, *et al.* A single arginine residue determines species specificity of the human growth hormone receptor. Proc Natl Acad Sci USA 1995;92:959–963.
27. Masumoto N, Tateno C, Tachibana A, *et al.* GH enhances proliferation of h-heps grafted into immunodeficient mice with damaged liver. J Endoclinol 2007;194:529–537.
28. Sandgren EP, Palmiter RD, Heckel JL, *et al.* Complete hepatic regeneration after somatic deletion of an albumin-plasminogen activator transgene. Cell 1991;66:245–256.
29. Dinchuk J, Hart J, Gonzalez G, *et al.* Remodelling of lipoproteins in transgenic mice expressing human cholesteryl ester transfer protein. Biochim Biophys Acta 1995;1255:301–310.

HEPATOLOGY
Official Journal of the American Association for the Study of Liver Diseases
AASLD

Adipose Tissue-Derived Stem Cells as a Regenerative Therapy for a Mouse Steatohepatitis-Induced Cirrhosis Model

Akihiro Seki,[1,2*] Yoshio Sakai,[1,3*] Takuya Komura,[2] Alessandro Nasti,[2] Keiko Yoshida,[2] Mami Higashimoto,[2] Masao Honda,[1] Soichiro Usui,[2] Masayuki Takamura,[2] Toshinari Takamura,[2] Takahiro Ochiya,[4] Kengo Furuichi,[5] Takashi Wada,[3] and Shuichi Kaneko[1,2]

Cirrhosis is a chronic liver disease that impairs hepatic function and causes advanced fibrosis. Mesenchymal stem cells have gained recent popularity as a regenerative therapy since they possess immunomodulatory functions. We found that injected adipose tissue-derived stem cells (ADSCs) reside in the liver. Injection of ADSCs also restores albumin expression in hepatic parenchymal cells and ameliorates fibrosis in a nonalcoholic steatohepatitis model of cirrhosis in mice. Gene expression analysis of the liver identifies up- and down-regulation of genes, indicating regeneration/repair and anti-inflammatory processes following ADSC injection. ADSC treatment also decreases the number of intrahepatic infiltrating $CD11b^+$ and $Gr\text{-}1^+$ cells and reduces the ratio of $CD8^+/CD4^+$ cells in hepatic inflammatory cells. This is consistent with down-regulation of genes in hepatic inflammatory cells related to antigen presentation and helper T-cell activation. *Conclusion*: These results suggest that ADSC therapy is beneficial in cirrhosis, as it can repair and restore the function of the impaired liver. (HEPATOLOGY 2013;58:1133-1142)

Cirrhosis is a serious, life-threatening advanced stage of chronic liver disease that leads to hepatic dysfunction.[1] Cirrhosis frequently develops into hepatocellular carcinoma,[2,3] which exacerbates the prognosis of patients with cirrhosis. The ultimate treatment for cirrhosis is a liver transplant,[4] which can be lethal.[5] The number of donor livers, however, is not sufficient to meet the needs of all transplant patients. Thus, a novel therapy for cirrhosis needs to be developed to improve cirrhotic liver prognosis.

The underlying pathogenesis of chronic liver disease is persistent inflammation. Advanced disease is marked by advanced fibrosis concomitant with distorted liver architecture characterized by regenerative nodules and impaired hepatic function. Advanced fibrosis in the cirrhotic liver is also a risk factor for the development of hepatocellular carcinoma.[6] Treatment of cirrhosis suppresses inflammation by eradicating hepatitis virus infection or reducing liver steatosis in nonalcoholic steatohepatitis (NASH). Decreasing liver inflammation and restoring hepatocyte function improves the prognosis.

Pluripotent mesenchymal stem cells (MSCs) differentiate into adipocyte, chondrocyte, and osteocyte lineages.[7] These cells can also differentiate into other lineages, including neurons[8] and hepatocytes.[9,10] MSCs can also regulate the immune response.[11] Thus, MSCs attract attention as a therapeutic target in the

Abbreviations: ADSCs, adipose-tissue-derived stem cells; AFP, alpha-fetoprotein; Ath+HF, atherogenic high-fat; IL, interleukin; MMP, matrix metalloproteinase; MSC, mesenchymal stem cells; NASH, nonalcoholic steatohepatitis; PBS, phosphate-buffered saline; 18S rRNA, 18S ribosomal RNA; α-SMA, alpha-smooth muscle actin.

From the [1]Department of Gastroenterology, Kanazawa University Hospital, Ishikawa, Japan; [2]Disease Control and Homeostasis, Kanazawa University, Ishikawa, Japan; [3]Department of Laboratory Medicine, Kanazawa University Hospital, Ishikawa, Japan; [4]National Cancer Research Institute, Tokyo, Japan; [5]Division of Blood Purification, Kanazawa University Hospital, Ishikawa, Japan.

Received September 27, 2012; accepted April 15, 2013.

Supported in part by subsidies from the Japanese Ministry of Education, Culture, Sports, Science and Technology and the Japanese Ministry of Health, Labor and Welfare.

[*]These authors contributed equally to this work.